



## RESEARCH ARTICLE

## Alterations in MRI-visible perivascular spaces precede dementia diagnosis by 18 years in autosomal dominant Alzheimer's disease

Riccardo Leone<sup>1,2,3</sup>  | Xenia Kobeleva<sup>1,3</sup> | Bryan Rowe<sup>4</sup> | Jeiran Choupan<sup>5,6</sup> | John M. Ringman<sup>4</sup> | Giuseppe Barisano<sup>7</sup> <sup>1</sup>Computational Neurology Group, Ruhr University Bochum, Bochum, Germany<sup>2</sup>Faculty of Medicine, University of Bonn, Bonn, Germany<sup>3</sup>German Center for Neurodegenerative Diseases (DZNE), Bonn, Germany<sup>4</sup>Department of Neurology, Keck School of Medicine, University of Southern California, Los Angeles, California, USA<sup>5</sup>Laboratory of Neuro Imaging (LONI), Mark and Mary Stevens Neuroimaging and Informatics Institute, Keck School of Medicine, University of Southern California, Los Angeles, California, USA<sup>6</sup>NeuroScope Inc., Scarsdale, New York, USA<sup>7</sup>Department of Neurosurgery, Stanford University, Stanford, California, USA

## Correspondence

Giuseppe Barisano, Department of Neurosurgery, Stanford University, 1201 Welch Road, Stanford, CA 94305, USA.  
Email: [barisano@stanford.edu](mailto:barisano@stanford.edu)

## Funding information

Alzheimer's Drug Discovery Foundation, Grant/Award Number: RC-202405-2026586; Helene and Lou Galen Professorship; National Institute on Aging, Grant/Award Numbers: K01AG22228, R01AG070825, R01AG062007, U01AG051218, P30AG066530, U19AG032438; National Institute of Mental Health, Grant/Award Number: RF1MH123223; National Institute of Neurological Disorders and Stroke, Grant/Award Number: R01NS128486; Alzheimer's Association, Grant/Award Number: SG-20-690363-DIAN; German Center for Neurodegenerative Diseases (DZNE); Raul Carrea Institute for Neurological Research (FLENI); Japan Agency for Medical Research and Development (AMED); Korea Health Industry Development Institute (KHIDI); Korea Dementia Research Center (KDRC); Ministry of Health &amp; Welfare and Ministry of Science ICT, Republic of Korea,

## Abstract

**INTRODUCTION:** Perivascular space (PVS) alterations are traditionally linked to cardiovascular risk factors and aging, but may also play a direct role in Alzheimer's disease (AD). To reduce confounding from age-related comorbidities, we examined PVSs in autosomal dominant AD (ADAD).**METHODS:** In this cross-sectional study of 96 non-demented individuals (62 mutation carriers), we quantified PVS count fraction and mean diameter in white matter and basal ganglia using automated magnetic resonance imaging analysis. Linear mixed models assessed group differences along the disease course, adjusting for cardiovascular risk factors.**RESULTS:** Compared to non-carriers, mutation carriers showed lower PVS count fraction in white matter and basal ganglia, and larger PVS diameter in basal ganglia and the temporal lobe. Changes were evident up to 18 years before expected dementia onset and followed trajectories similar to amyloid beta 42 and tau biomarkers.**DISCUSSION:** ADAD is associated with early PVS alterations, suggesting perivascular changes may be integral to primary AD pathology.

## KEYWORDS

Alzheimer's disease, autosomal dominant Alzheimer's disease, cerebral small vessel disease, dominantly inherited Alzheimer's disease, magnetic resonance imaging, perivascular spaces

This is an open access article under the terms of the [Creative Commons Attribution-NonCommercial-NoDerivs](https://creativecommons.org/licenses/by-nc-nd/4.0/) License, which permits use and distribution in any medium, provided the original work is properly cited, the use is non-commercial and no modifications or adaptations are made.© 2025 The Author(s). *Alzheimer's & Dementia* published by Wiley Periodicals LLC on behalf of Alzheimer's Association.

Grant/Award Number: RS-2024-00344521;  
Spanish Institute of Health Carlos III (ISCIII)

### Highlights

- Autosomal dominant Alzheimer's disease (ADAD) mutation carriers have reduced magnetic resonance imaging–visible perivascular space (PVS) count fraction in the white matter and basal ganglia.
- ADAD mutation carriers show enlarged PVS in the basal ganglia and temporal white matter.
- PVS alterations start 18 years before the estimated time of dementia diagnosis.
- The spatial localization of PVS changes overlaps with regions of amyloid beta ( $A\beta$ ) accumulation.
- The temporal evolution of PVS alterations aligns with  $A\beta$  and tau changes in the cerebrospinal fluid.

## 1 | BACKGROUND

Cerebral small vessel disease (CSVD) is frequently observed in association with Alzheimer's disease (AD) pathology in *post mortem* analyses of individuals with late-onset AD<sup>1</sup> (LOAD), and may represent a significant contributor to neurodegeneration and cognitive impairment.<sup>2</sup> Similarly, in vivo neuroimaging markers of CSVD, such as white matter lesions (WMLs), lacunes, and perivascular space (PVS) alterations, often co-occur with abnormalities of AD biomarkers in elderly individuals.<sup>3–5</sup> However, CSVD markers are strongly associated with aging and cardiovascular risk factors. Therefore, whether the involvement of small brain vessels is an intrinsic component of AD pathogenesis or an independent pathological process is still unclear.

Autosomal dominant AD (ADAD)—a genetic form of AD determined by fully penetrant mutations in the genes coding for amyloid precursor protein (APP), presenilin 1 (PSEN1), or presenilin 2 (PSEN2)—provides a unique model for studying AD pathogenesis. ADAD mutations appear to cause disease through aberrant metabolism of amyloid beta ( $A\beta$ ), leading to excessive production of long forms of  $A\beta$ .<sup>6</sup> Individuals with ADAD typically develop symptoms from a younger age (30–50 years),<sup>7</sup> when the confounding effects of aging and cardiovascular risk factors on brain pathology are limited. Additionally, the highly heritable age of symptom development in ADAD<sup>7</sup> allows one to approximate the estimated disease trajectory, which can be used as a reference to evaluate the timing of AD biomarker changes.<sup>8–12</sup> Identifying evidence of CSVD biomarker changes in ADAD would strongly suggest that they reflect primary AD-related pathological mechanisms rather than mechanisms secondary to aging or vascular comorbidities.

To date, a few studies have investigated WML in individuals with ADAD, reporting higher WML volume in mutation carriers compared to non-carriers.<sup>9,13,14</sup> Other vascular-related neuroimaging markers, such as PVS, remain understudied in ADAD. PVS are fluid-filled tubular spaces surrounding cerebral blood vessels, especially within the white matter (WM) and basal ganglia (BG).<sup>15</sup> PVS visibility on magnetic resonance imaging (MRI) depends on the presence of fluid within

PVS,<sup>16</sup> which is driven by arterial pulsatility and vasomotion.<sup>17–21</sup> Current methods allow us to obtain whole-brain quantitative measures regarding the count and diameter of MRI-visible PVS in vivo, improving sensitivity in detecting subtle and early PVS alterations.<sup>5</sup> While the pathophysiology underlying PVS alterations remains unclear, it was proposed that blood–brain barrier breakdown, arteriosclerosis, cerebral amyloid angiopathy (CAA), and/or glymphatic impairment may lead to alterations in fluid flow through PVS and subsequent modifications of PVS structure.<sup>22</sup> Previous *post mortem* studies in ADAD have described a higher prevalence of CAA<sup>23</sup> and other indices of cerebrovascular disease.<sup>24</sup> However, only one *post mortem* study investigated PVS in ADAD, reporting enlarged PVS diameter and suggesting that AD-specific mechanisms might involve the perivascular compartment.<sup>25</sup> In vivo evidence for PVS structural alterations in ADAD is lacking, and the regional and temporal course of these pathophysiological alterations remains unexplored.

In this study, we used a robust, fully automated, and clinically feasible MRI-based approach for PVS quantification,<sup>5</sup> to investigate, in vivo, PVS characteristics in ADAD mutation carriers versus non-carriers. We focused on two previously established markers of PVS pathology,<sup>5</sup> namely, PVS count fraction (i.e., the number of PVSs in a brain region divided by its volume), and PVS mean diameter. Lower PVS count and higher PVS diameter have recently been associated with increased risk of incident dementia and accelerated neurodegeneration in elderly individuals.<sup>5</sup> We thus hypothesized that mutation carriers would have a reduced PVS count fraction and increased PVS mean diameter, and that between-group changes in these biomarkers would be noticeable before dementia diagnosis. Furthermore, we also compared the observed trajectories of PVS changes to those of other well-established AD biomarkers.

Identifying novel in vivo pathologic features in ADAD, such as PVS alterations, has the potential to provide new insights into the pathophysiology of AD, to improve early diagnosis and monitoring of disease progression, and to offer new opportunities for the development of preventative or treatment strategies.

## 2 | METHODS

### 2.1 | Participants

We performed a retrospective cross-sectional analysis of individuals enrolled in prior and ongoing studies of ADAD being conducted by principal investigator J. M. Ringman. The data analyzed in this study were acquired between June 2005 and July 2022. Each participant was a member of a pedigree with a known mutation for ADAD in the *APP*, *PSEN1*, or *PSEN2* genes. Given the small number of participants at risk for inheriting *PSEN2* mutations, we treated *PSEN1* and 2 mutations together as a single *PSEN* group.

Though prior studies use parental- or mutation-based estimates of the age of symptom onset,<sup>9,26,27</sup> we have found variability among family members with regard to the report of symptom onset. More reliable is the age of dementia diagnosis, namely the age at which affected family members meet criteria for dementia by history. A mean age of dementia diagnosis was calculated for each mutation based on family member reports and the published literature (Table S1 in supporting information).<sup>7</sup> We calculated the estimated years from dementia diagnosis (EDD) by subtracting from the participant's age the expected age of dementia diagnosis associated with the mutation they were at risk for inheriting. Based on data freeze 17 of the Dominantly Inherited Alzheimer Network (DIAN) dataset, the average difference between the DIAN-determined age of first symptom onset and our determined age of dementia diagnosis is  $\approx 2.6$  years.

We gathered data from 121 subjects with available MRI and clinical information obtained during the same visit. We limited our analyses to subjects without dementia, as defined by having a Clinical Dementia Rating scale score  $\leq 1$  and assessed before their expected age of dementia diagnosis ( $EDD \leq 0$ ). This choice was performed to focus on the earliest stages of the disease to avoid potential confounding effects due to severe brain atrophy, which could bias estimations of PVS. Ninety-six subjects met the inclusion criteria and had full availability of clinical covariates of interest (see next section). All participants or their caregivers provided informed consent.

### 2.2 | Covariates of interest

Covariates of interest included EDD; reported sex; history of hypertension, hypercholesterolemia, and diabetes; apolipoprotein E (*APOE*) genotype; and mutation status. *APOE* status was coded categorically (presence or absence of an  $\epsilon 4$  allele). Cardiovascular risk was quantified by summing scores for hypertension, hyperlipidemia, and diabetes presence (1 point for each risk factor, total range: 0–3).

### 2.3 | MRI data acquisition and processing

Brain MRI was performed on 1.5 Tesla ( $N = 13$ ), or 3 Tesla ( $N = 83$ ) Siemens scanners using T1-weighted magnetization-prepared rapid gradient echo (MPRAGE) sequence (parameters in Table S2 in

#### RESEARCH IN CONTEXT

- 1. Systematic review:** We conducted a systematic review of PubMed through December 1, 2024, and found only one prior *post mortem* study reporting enlarged perivascular spaces (PVSs) in autosomal dominant Alzheimer's disease (ADAD).
- 2. Interpretation:** Whether PVS alterations reflect primary Alzheimer's disease (AD) pathology or age-related vascular comorbidities remains unclear. Here, we provide the first in vivo evidence that ADAD mutation carriers exhibit significantly lower PVS count fraction in the white matter and basal ganglia, alongside increased PVS diameter in the basal ganglia and temporal lobe, compared to non-carriers. These differences emerged up to 18 years before expected dementia onset and followed a temporal and spatial trajectory similar to established AD biomarkers such as amyloid beta and tau. PVS alterations were independent of cardiovascular risk factors.
- 3. Future directions:** Our findings support a direct involvement of the vascular/perivascular compartment in ADAD pathophysiology and suggest that magnetic resonance imaging-visible PVSs may serve as an early, accessible biomarker of disease progression.

supporting information). All imaging analyses were completed with fully automated algorithms without knowledge of mutation status, or demographic or clinical data.

Images were preprocessed and resampled to 1 mm isotropic resolution with FreeSurfer v7.4,<sup>28</sup> as previously described.<sup>5</sup> PVS were automatically segmented on preprocessed T1-weighted images in the whole-brain normal appearing WM (obtained by subtracting the WML voxels from the WM mask), and in the BG. The PVS segmentation method enhances vessel-like structures by applying a Frangi filter,<sup>29</sup> which assigns a "vesselness" value based on the eigenvalues of the Hessian matrix. The value of the 85th percentile of the total number of voxels with non-zero "vesselness" is used as a threshold, and only voxels with a "vesselness" value above this threshold are retained and binarized to generate a PVS mask. MATLAB's "regionprops3" was used to compute count and mean diameter across all PVS clusters with an in-plane size of at least 2 voxels in each region. PVS count was standardized by the volume of each region, yielding a PVS count fraction, as per previous recommendations.<sup>16</sup> Both PVS metrics have excellent intraclass correlation coefficients ( $\geq 0.9$  for WM-PVS and  $\geq 0.8$  for BG-PVS) regarding inter-scanner reproducibility, interfield-strength reproducibility, and test-retest repeatability.<sup>5</sup> We also performed exploratory analyses considering PVS characteristics in the normal-appearing WM of each brain lobe (frontal, parietal, temporal, insular, and occipital), as parcellated with FreeSurfer v7.4.<sup>28</sup> Values were averaged between the left and right hemispheres before further

analysis. WML were segmented on preprocessed T1-weighted images with a fully automated algorithm,<sup>30</sup> robust in terms of interscanner and test–retest reproducibility, and whose results strongly correlated with those obtained from fluid-attenuated inversion recovery (FLAIR) sequences.<sup>5</sup>

All segmentation masks were visually checked for accuracy in a blinded fashion by an expert physician scientist (G.B., 10 years of experience in neuroimaging). Individual PVS segmentations for all subjects are available at <https://gbarisano.shinyapps.io/pvs-dementia/> (select project: “Autosomal Dominant Alzheimer Disease – EEAJ”).

## 2.4 | Statistical analysis

Descriptive statistics are presented for categorical data as numbers (percentages) and for continuous data as mean  $\pm$  standard deviation for normally distributed variables, or as median (interquartile range) for not-normally distributed variables. Categorical variables were compared between the mutation status group based on the chi-squared test, while continuous variables were compared with the two-sample independent *t* test or Mann–Whitney *U* test for normally and not-normally distributed variables, respectively.

A linear mixed model, with family membership as a random factor,<sup>8</sup> was used to estimate the association of mutation status versus PVS count fraction or PVS mean diameter as dependent variables in each considered region. Analyses were adjusted for EDD and its interaction with mutation status, cardiovascular risk, APOE status, and sex, as fixed factors. A similar model was also run with WML volume (log-transformed) as the dependent variable. Total intracranial volume was not significantly associated with PVS metrics nor with WML and was not included as a covariate (Figure S1 in supporting information). Following previous studies,<sup>8,31</sup> we assessed PVS biomarker differences at various age points using an approximate Student *t* test on results derived from linear mixed models. This allowed us to assess the trajectories of PVS changes over time and to identify the time point of the first significant differences between groups.

Most subjects lacked cerebrospinal fluid (CSF) and positron emission tomography (PET) imaging data. Given the highly heritable age of symptom development in ADAD, which allows one to approximate the estimated disease trajectory,<sup>7</sup> we compared PVS metrics to other well-established biomarkers of ADAD using data from Bateman et al.<sup>8</sup> These data represent the standardized differences in each biomarker between mutation carriers and non-carriers as a function of estimated years from symptom onset (EYO). To reconcile the difference between the definition of EYO used in Bateman et al.<sup>8</sup> and our definition of EDD, we added 2.6 years—the average time difference between DIAN-determined EYO and our-determined EDD—to EDD and used this surrogate EYO when comparing our PVS metrics with the other ADAD biomarkers. Following Bateman et al.,<sup>8</sup> we calculated estimates for PVS metrics using the previously described linear mixed models.

A *p* value of  $< 0.05$  was considered statistically significant for analyses of WM or BG. Exploratory analyses were also performed for each brain lobe.

**TABLE 1** Subject characteristics divided by the presence or absence of mutations leading to autosomal dominant Alzheimer's disease.

	Non-carriers (n = 34)	Carriers (n = 62)	<i>p</i> value
Age	35.0 (28.2 - 39.0)	32.5 (26.2–41.8)	0.930
EDD (years)	−15.32 $\pm$ 9.83	−13.32 $\pm$ 8.34	0.319
WML volume (log)	1.8 (0.0 - 2.3)	2.3 (1.8–2.6)	<b>0.006</b>
Sex			0.91
Male	12 (35.29%)	24 (38.71%)	
Female	22 (64.71%)	38 (61.29%)	
APOE $\epsilon$ 4+ (%)			1.00
0	26 (76.47%)	48 (77.42%)	
1	8 (23.53%)	14 (22.58%)	
CV risk (%)			0.12
0	26 (76.47%)	54 (87.1%)	
1	8 (23.53%)	6 (9.68%)	
2	0 (0.0%)	2 (3.23%)	
Gene (%)			1.00
APP	7 (20.59%)	12 (19.35%)	
PSEN1/2	27 (79.41%)	50 (80.65%)	

Note: Categorical data are reported as a number (percentages), and the corresponding *p* value refers to differences between the mutation status groups based on the chi-squared test. Continuous data are reported as mean  $\pm$  standard deviation for normally distributed variables or as median (interquartile range) for variables that are not normally distributed. Corresponding *p* value refers to the two-sample independent *t* test or Mann–Whitney *U* test for normally and not normally distributed variables, respectively. Statistically significant comparisons are highlighted in bold. Abbreviations: ADAD, Autosomal dominant Alzheimer's disease; APOE, apolipoprotein E; APP, amyloid precursor protein; CV, cardiovascular; EDD, estimated years from dementia diagnosis; PSEN, presenilin; WML, white matter lesion.

## 3 | RESULTS

We analyzed data from 96 subjects (median age: 33 [interquartile range: 27–40], 62.5% females). Among them, 62 (64.6%) were carriers of ADAD mutations: 50 (80.6%) had *PSEN* mutations and 12 (19.4%) had *APP* mutations (Table 1). In unadjusted comparisons, mutation carriers showed a significantly greater volume of WML ( $p = 0.006$ ). After adjusting for other covariates in a linear mixed model, no significant associations between WML volume and mutation status were found ( $p = 0.18$ , Table S3 in supporting information). There were no other significant differences between groups in clinical or demographic variables. In mutation carriers, the BG–PVS count fraction was significantly correlated with WM–PVS count fraction, as well as with regional values in the frontal and insular lobes. Similarly, the mean BG–PVS diameter showed significant correlations with mean WM–PVS diameter in the white matter and in all cortical lobes except the occipital lobe (Table S4 in supporting information).

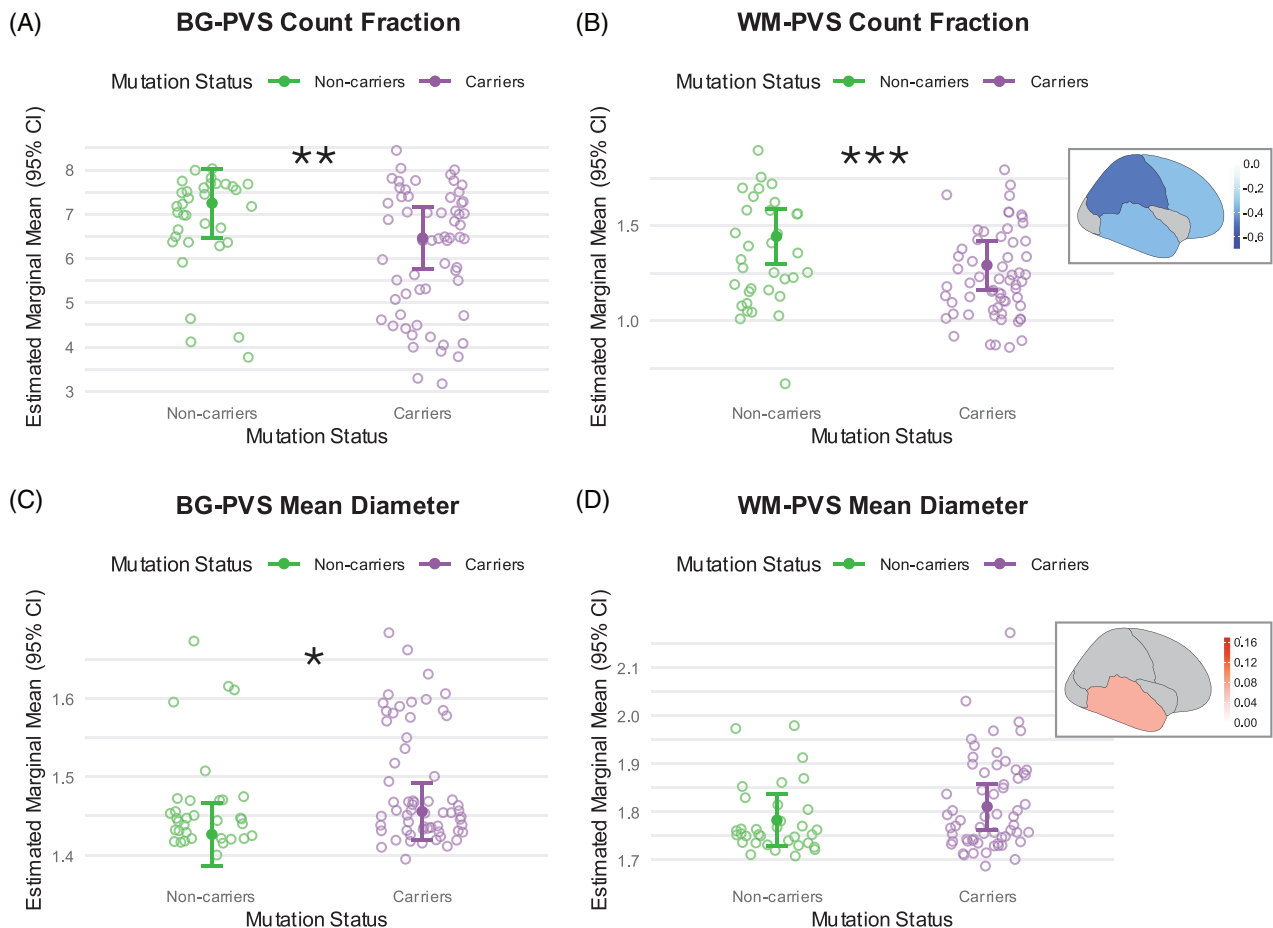


**FIGURE 1** Differences in perivascular space count fraction and mean diameter in the white matter and basal ganglia. Estimated marginal means (solid dots) and 95% confidence intervals (error bars) for PVS count fraction (A, B) and PVS mean diameter (C, D) in non-carriers (green) and mutation carriers (violet) in the BG (A, C) and WM (B, D). Mean estimates were obtained using linear mixed models including mutation status, estimated years from dementia diagnosis, and their interaction; sex, cardiovascular risk score; and presence of an APOE  $\epsilon 4$  allele as fixed effects, while family membership was included as a random effect. Empty colored dots correspond to individual empirical observations. The asterisk(s) refer to the  $p$  value for the variable "mutation status" obtained from the adjusted linear mixed model. Insets in (B) and (D) show color-coded brain maps illustrating model coefficients for "mutation status" in various brain regions against PVS count fraction or PVS mean diameter, respectively. Cooler colors (e.g., darker blue) represent regions with stronger negative associations, while warmer colors (e.g., red) indicate regions with stronger positive associations between mutation status and PVS biomarkers. Only regions with uncorrected  $p$  value  $< 0.05$  are shown, while others are grayed out. \*:  $0.01 \leq p < 0.05$ ; \*\*:  $0.001 \leq p < 0.01$ ; \*\*\*:  $0.0001 \leq p < 0.001$ . APOE, apolipoprotein E; BG, basal ganglia; CI, confidence interval; PVS, perivascular space; WM, white matter.

We first estimated overall differences in PVS metrics in mutation carriers compared to non-carriers (Figure 1, Table S3). Mutation carriers showed significantly lower PVS count fraction in the WM ( $\beta = -0.33$ , 95% confidence interval [CI]:  $-0.5$  to  $-0.17$ ,  $p = 0.00013$ )—particularly in the frontal, parietal, and temporal lobes (exploratory regional analyses summarized in Table S5 in supporting information)—and in the BG ( $\beta = -1.5$ , 95% CI:  $-2.4$  to  $-0.65$ ,  $p = 0.0011$ ). PVS mean diameter was significantly higher in mutation carriers versus non-carriers in the BG ( $\beta = 0.055$ , 95% CI:  $0.0093$  to  $0.10$ ,  $p = 0.021$ ), but not across the whole WM ( $\beta = 0.034$ , 95% CI:  $-0.028$  to  $0.097$ ,  $p = 0.28$ ). In exploratory analyses at a lobar level, PVS mean diameter was greater in the temporal lobe of carriers versus non-carriers (Table S5). We observed significant positive associations between BG and WM-PVS count fraction and EDD. This association is analogous to the estab-

lished positive association between PVS count fraction and increasing chronological age observed in adults.<sup>32</sup> However, this positive association with EDD was significantly modified by mutation status, as indicated by a negative interaction effect (Table S3). While non-carriers exhibited the expected increase in BG and WM-PVS count fraction with increasing EDD,<sup>32</sup> the negative interaction effect resulted in a significant decrease in PVS count fraction with increasing EDD among mutation carriers (Table 2). We confirmed the known positive association between WM-PVS count fraction and male sex,<sup>5,32</sup> and found a significant negative association between mean BG-PVS diameter and APOE status (Table S3).

Next, following Bateman et al.<sup>8</sup> and Araque Caballero et al.,<sup>31</sup> we estimated differences in PVS count fraction between carriers and non-carriers at various time cut-offs (Figure 2, Table 2). This allowed us to



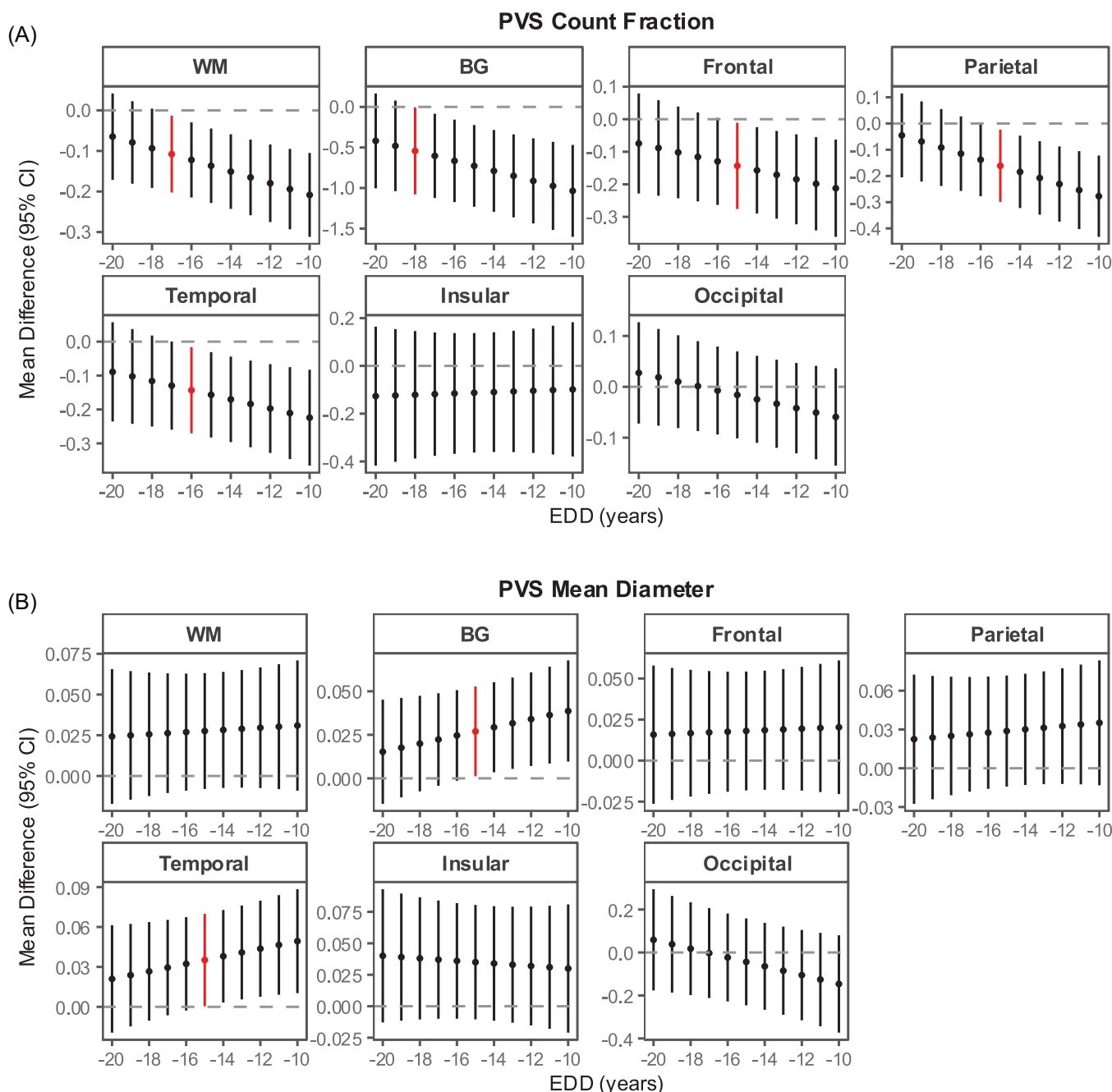


**FIGURE 2** Time of first detectable changes in perivascular spaces count fraction and mean diameter. Mean and 95% confidence intervals of the estimated differences in PVS count fraction (A) and mean diameter (B) between mutation carriers and non carriers. Differences were calculated with linear mixed models at each estimated year from EDD (range: -20 to -10). Linear mixed models included mutation status, EDD, and their interaction; sex; cardiovascular risk score; and presence of APOE  $\epsilon 4$  allele(s) as fixed effects, while family membership was included as a random effect. Estimated mean differences were averaged over levels of cardiovascular risk, sex, and APOE. The red bar indicates the earliest time point of abnormal PVS metrics for a particular brain region. APOE, apolipoprotein E; BG, basal ganglia; CI, confidence interval; EDD, expected dementia diagnosis; PVS, perivascular space; WM, white matter.

identify the earliest timepoint at which significant differences in PVS biomarkers were first observed in carriers compared to non-carriers. We observed the first significant reductions in PVS count fraction at -18 years before EDD in the BG and at -17 years in the WM (Table S6 in supporting information). The first significant increase in BG-PVS mean diameter was seen -15 years before EDD. Regional estimates of

between-group differences in PVS biomarkers highlighted early reductions in PVS count fraction in the temporal, frontal, and parietal lobes, as well as early PVS enlargement in the temporal lobe (Figure 2, Table S6 and S7 in supporting information).

Then, we compared how PVS alterations evolve over time in relation to changes of other well-established AD biomarkers (Figure 3).

**TABLE 2** Perivascular spaces metrics estimates in mutation carriers versus non-carriers.

		Estimated years from dementia diagnosis					
Variable	Region	−25	−20	−15	−10	−5	0
PVS count fraction							
Non-carriers	WM	1.34	1.39	1.43	1.48	1.53	1.58
Carriers	WM	1.34	1.32	1.30	1.27	1.25	1.23
Difference	WM	0.01±0.14	−0.06±0.11	−0.14±0.09	−0.21±0.10	−0.28±0.13	−0.35±0.18
Non-carriers	BG	7.12	7.18	7.24	7.30	7.36	7.42
Carriers	BG	7.01	6.76	6.51	6.26	6.01	5.77
Difference	BG	−0.11±0.77	−0.42±0.59	−0.73±0.5	−1.04±0.57	−1.34±0.74	−1.65±0.96
PVS mean diameter							
Non-carriers	WM	1.76	1.77	1.78	1.79	1.80	1.81
Carriers	WM	1.78	1.80	1.81	1.82	1.83	1.84
Difference	WM	0.02±0.05	0.02±0.04	0.03±0.04	0.03±0.04	0.03±0.05	0.04±0.07
Non-carriers	BG	1.435	1.431	1.427	1.423	1.420	1.416
Carriers	BG	1.438	1.446	1.454	1.462	1.470	1.478
Difference	BG	0.004±0.039	0.015±0.03	0.027±0.026	0.039±0.029	0.05±0.038	0.062±0.049

Note: Estimates of mean PVS count fraction and mean diameter in the WM and BG at various age cut-offs were calculated using the estimated years from dementia diagnosis. Difference refers to the estimated difference between mutation carriers and non-carriers ± 95% confidence intervals. Reported estimates were obtained using a linear mixed model with mutation status (non-carrier or carrier), expected years from dementia diagnosis, and their interaction, cardiovascular risk score, presence of an APOE ε4 allele, and sex as fixed effects. Family membership was considered a random effect. Results were averaged over levels of cardiovascular risk, sex, and APOE. For regional estimates in the WM, see Table S5 in supporting information. Note that there might be small discrepancies in differences due to rounding.

Abbreviations: APOE, apolipoprotein E; BG, basal ganglia; PVS, perivascular spaces; WM, white matter.

Using data from a previous study by Bateman et al.<sup>8</sup> for this comparison, we found that the initial changes and following time course of PVS count fraction reduction and BG–PVS enlargement closely aligned with reported changes in Aβ and tau in the CSF (Figure 3).

Finally, we compared PVS characteristics between carriers of APP and PSEN mutations. We found no statistically significant differences in PVS metrics, except for a lower PVS count fraction in the temporal lobe of PSEN carriers compared to APP carriers ( $p = 0.003$ , Figure S2 in supporting information).

## 4 | DISCUSSION

We found significant PVS alterations in carriers of pathogenetic mutations for ADAD compared to non-carrier family members. The first differences occurred as early as 18 years before the expected age of dementia diagnosis. The timeframe of initial PVS changes and their trajectory along the estimated disease course aligned with those of Aβ and tau pathology in the CSF previously reported in ADAD<sup>8</sup> and LOAD.<sup>33</sup> The spatial localization of PVS changes also overlapped with regions of known early pathology in ADAD.<sup>8,10,34</sup> Between-group differences in PVS metrics became more prominent as the disease progressed, suggesting that PVS alterations may contribute to ensuing neurodegeneration and the development of symptoms. Given the young age of the analyzed individuals and the independence of these results from cardiovascular risk factors, our findings suggest that alterations

in MRI-visible PVS might indicate pathological processes occurring in the small cerebral vessels and/or their perivascular compartments that are specifically related to AD pathophysiology rather than other comorbidities.

We found that mutation carriers had significantly lower PVS count fraction in the BG and WM compared to non-carriers. It is important to note that our PVS count fraction differs from the conventional count of PVS in visual rating scales performed by human raters. Traditional visual rating methods typically assess the number of visibly enlarged PVS in one hemisphere within a single representative MRI slice. This approach provides only a partial view of PVS burden, may depend on the rater performing the evaluation, and lacks sensitivity to smaller or non-enlarged PVS. Moreover, visual rating scales typically do not account for total or regional brain volume, despite evidence that PVS counts are associated with brain volume.<sup>16</sup> In contrast, our fully automated segmentation method quantifies all MRI-visible PVS across the entire brain, irrespective of their enlargement status. This allows us to perform a complete quantitative analysis, also incorporating blood vessels with small/non-enlarged perivascular space.<sup>5</sup> Moreover, by using PVS count fraction (number of PVS divided by regional volume) in all our analyses, we corrected for brain volume as a potential confounder. Our approach thus enables a more sensitive, comprehensive, accurate, and reproducible characterization of overall PVS characteristics compared to visual rating scales.<sup>5</sup>

PVS are considered a marker of CSVD,<sup>15</sup> and their visibility on MRI depends on the presence of fluid within the perivascular

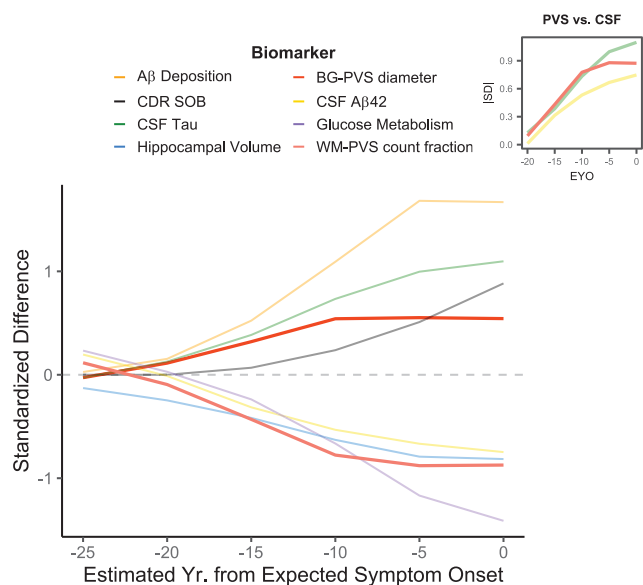


**FIGURE 3** Changes in clinical, imaging, and biochemical biomarkers with respect to changes in perivascular space metrics as a function of estimated years from expected symptom onset. The main panel displays the SD between mutation carriers and non carriers over the expected course of the disease for various clinical, imaging, and biochemical biomarkers, as reported in Bateman et al. These differences are compared to the SD in PVS count fraction in the WM (WM-PVS count fraction, in tight red) and PVS mean diameter in the BG (BG-PVS mean diameter, in red). The expected course of the disease is assessed using the estimated years from EYO. To reconcile the discrepancy between the definition of EYO onset used in Bateman et al. and our definition of EDD, we added 2.6 years to EDD before estimating SD for PVS metrics. This number represented the average time difference between DIAN-determined EYO and our-determined EDD (see main text). The inset highlights the comparison between WM-PVS count fraction and CSF biomarkers ( $A\beta$  and tau). To facilitate visual comparisons of the relative magnitude and temporal course of changes, absolute values of SDs are shown.  $A\beta$ , amyloid beta; BG, basal ganglia; CDR-SOB, Clinical Dementia Rating Sum of Boxes; CSF, cerebrospinal fluid; DIAN, Dominantly Inherited Alzheimer Network; EDD, expected dementia diagnosis; EYO, expected symptom onset; PVS, perivascular space; SD, standardized differences; WM, white matter.

compartment,<sup>16</sup> and on its flow, which is driven by arterial pulsatility and vasomotion.<sup>17,18,20</sup> Although the exact pathophysiology underlying reduced PVS visibility on MRI is still not fully elucidated, impaired arterial pulsatility has been associated with reduced PVS fluid flow,<sup>19,21</sup> and a lower PVS count has been associated with cerebral hypoperfusion.<sup>5</sup> Given these associations, the reduction in PVS count fraction observed in mutation carriers may reflect early AD-related small vessel pathology. This interpretation is supported by previous findings of CSVD in *post mortem* ADAD cases,<sup>25</sup> lower cerebral blood flow in ADAD,<sup>35</sup> and reduced microvascular density in Down syndrome,<sup>36</sup> a condition characterized by overexpression of the APP gene linked with increased brain amyloid levels and early-onset AD. This suggests that the genetic underpinnings of ADAD might lead to early vascular changes, potentially affecting perivascular fluid flow, and

consequently, reducing the MRI visibility of PVS. Consistently, recent studies of PVS in LOAD have also found lower PVS amount across multiple brain regions in patients with mild cognitive impairment or before the development of dementia compared to cognitively unimpaired and stable subjects.<sup>5,37</sup>

PVS are increasingly recognized as a crucial component of the brain's glymphatic system, which is responsible for the clearance of metabolites, interstitial fluid, and waste from the brain.<sup>16,22,38</sup> Accumulation of misfolded proteins within PVS might impede fluid flow,<sup>39</sup> contributing to the observed reduction in MRI-visible PVS. The earliest significant reductions in PVS count fraction occurred in the BG and WM  $\approx 18$  years before the estimated onset of dementia and increased over time. Specifically, while non-carriers exhibited the expected increase in BG and WM-PVS count fraction with increasing age (as represented by EDD),<sup>32</sup> mutation carriers showed reductions in PVS count over time. The trajectory of between-group PVS changes aligned temporally with differences in  $A\beta_{1-42}$  and tau in the CSF.<sup>8,11</sup> Reductions in PVS count fraction were prominent in the basal ganglia and parietal, temporal, and frontal lobes. These regions are well known to exhibit early and elevated deposition of  $A\beta$  in ADAD.<sup>8,10,34</sup> Collectively, these results suggest a potential interplay between PVS and  $A\beta$  pathology. Impaired perivascular drainage, potentially exacerbated by  $A\beta$  accumulation within the perivascular compartment and/or vessel walls (i.e., CAA), could compromise fluid flow along PVS,<sup>40</sup> possibly creating a pathogenic feedback loop. Prior neuropathological studies have shown a higher prevalence of CAA in *post mortem* cases of ADAD,<sup>23,24</sup> but the precise timing of its development remains to be elucidated.

We observed significantly enlarged PVS in mutation carriers compared to non-carriers, especially within the BG and temporal WM. This finding provides *in vivo* corroboration for previous *post mortem* reports indicating PVS enlargement in individuals with ADAD.<sup>25</sup> The co-occurrence and temporal sequence of reduced PVS count and enlarged PVS diameter warrant careful consideration of the underlying mechanisms. One possibility is that these two phenomena may be pathologically linked. The reduction in the number of MRI-detectable PVS might relate to the obstruction of perivascular pathways. This could lead to a compensatory redistribution and accumulation of perivascular fluid in the remaining patent spaces, which might drive their progressive enlargement over time. This interpretation, although speculative, is supported by our findings that PVS enlargement emerged later than the initial reduction in count fraction,  $\approx 15$  years before the expected onset of dementia. Alternatively, mechanisms not directly associated with  $A\beta$  might drive PVS enlargement. For example, the timeframe of PVS enlargement parallels that of alterations of a secreted form of triggering receptor expressed on myeloid cells 2—a surrogate marker for microglial activation—in the CSF,<sup>41</sup> suggesting a potential role for inflammatory infiltrates.<sup>42–44</sup> Additionally, PVS enlargement in ADAD has been associated with reductions in astrocytic aquaporin-4, in the absence of CAA.<sup>25</sup> In this regard, we found a negative association between mean BG-PVS diameter and the presence of an APOE  $\epsilon 4$  allele. This may lend some further support to the hypothesis that PVS enlargement, at least in this region, may occur due to processes distinct from CAA, given that APOE  $\epsilon 4$  is a known risk factor for



CAA.<sup>45</sup> Previous findings on the association between PVS enlargement and APOE  $\epsilon$ 4 have been mixed, ranging from null results<sup>46,47</sup> to significant PVS enlargement only in the presence of two copies of the  $\epsilon$ 4 allele.<sup>5</sup> Future research is needed to further elucidate the influence of APOE genotypes on PVS enlargement. Last, in our ADAD cohort, we observed similar associations and significant correlations between PVS metrics in the BG and in several WM regions. While previous literature often emphasizes a clear dichotomy between BG and WM PVS alterations in older adults—typically linking them to distinct vascular pathologies—our findings support the notion that in the context of ADAD, PVS alterations may reflect a shared and AD-specific pathological mechanism.

Our study has some limitations, including its cross-sectional nature. Nonetheless, ADAD is characterized by a stereotypical pattern of pathological progression, with a predictable age of symptoms and dementia onset.<sup>8</sup> Therefore, the use of EDD allowed us to assess the evolution of PVS changes along the estimated trajectory of the disease. Another limitation is the lack of other AD biomarkers, such as amyloid and tau CSF or PET data. Thus, we could only indirectly compare how the trajectories of PVS changes relate to other AD biomarkers based on previously published data. Future longitudinal studies are needed to better evaluate the coupled temporal dynamics between PVS and other AD biomarker changes in the same individuals. Additionally, regional analyses were exploratory, aiming to identify specific locations with greater PVS changes. Consequently, these findings should be interpreted with caution as hypothesis generating. However, they provide a foundation for targeted, confirmatory investigations in independent cohorts of individuals with ADAD.

In conclusion, ADAD mutation carriers show early alterations in PVS characteristics in the WM and BG. These PVS alterations may be specific for AD-associated processes and not related to cardiovascular risk factors. Given the early involvement in the disease, the regional distribution of changes, and the hypothesized co-localization of several pathological mechanisms at/near PVS, our findings point to PVS as a relevant hub of pathology in ADAD. If confirmed in future longitudinal studies, this evidence could support research for preventative or treatment strategies targeting the vascular/perivascular compartment in ADAD. Furthermore, given the need for only a 3D T1-weighted MRI sequence, which is commonly acquired in clinical and research MRI protocols, our PVS metrics might be promising non-invasive and inexpensive candidate biomarkers to monitor disease course in ADAD.

## ACKNOWLEDGMENTS

We acknowledge the altruism of the participants and their families and contributions of the DIAN research and support staff at each of the participating sites for their contributions to this study. This study was supported by grant RC-202405-2026586 from the Alzheimer's Drug Discovery Foundation to G.B., and by NIA K01AG22228, R01AG062007, U01AG051218, P30AG066530, and the Helene and Lou Galen Professorship to J.M.R. J.C. is supported by grants RF1MH123223, R01AG070825, and R01NS128486 from the NIH. Data collection and sharing for this project was supported by The Dominantly Inherited Alzheimer Network (DIAN, U19AG032438) funded by the National

Institute on Aging (NIA), the Alzheimer's Association (SG-20-690363-DIAN), the German Center for Neurodegenerative Diseases (DZNE), Raul Carrea Institute for Neurological Research (FLENI), and partial support by the Research and Development Grants for Dementia from Japan Agency for Medical Research and Development (AMED), the Korea Health Technology R&D Project through the Korea Health Industry Development Institute (KHIDI), Korea Dementia Research Center (KDRC), funded by the Ministry of Health & Welfare and Ministry of Science and ICT, Republic of Korea RS-2024-00344521, and Spanish Institute of Health Carlos III (ISCIII). This manuscript has been reviewed by DIAN Study investigators for scientific content and consistency of data interpretation with previous DIAN Study publications. The founding sources had no role in study design; in the collection, analysis, and interpretation of data; in the writing of the report; nor in the decision to submit the article for publication.

## CONFLICT OF INTEREST STATEMENT

The authors declare no conflicts of interest. J.C. receives salary from a startup company, NeuroScope Inc. G.B. is listed as an inventor on a patent application related to this work filed by Stanford University, with no financial interest/conflict. All other authors declare no competing interests. Author disclosures are available in the [supporting information](#).

## CONSENT STATEMENT

All participants or their caregivers provided informed consent.

## ORCID

Riccardo Leone  <https://orcid.org/0000-0001-5569-6090>

Giuseppe Barisano  <https://orcid.org/0000-0001-5598-1369>

## REFERENCES

- Karant S, Nelson PT, Katsumata Y, et al. Prevalence and clinical phenotype of quadruple misfolded proteins in older adults. *JAMA Neurol*. 2020;77(10):1299-1307. doi:10.1001/jamaneurol.2020.1741
- Wardlaw JM, Smith C, Dichgans M. Small vessel disease: mechanisms and clinical implications. *Lancet Neurol*. 2019;18(7):684-696. doi:10.1016/S1474-4422(19)30079-1
- Graff-Radford J, Arenaza-Urquijo EM, Knopman DS, et al. White matter hyperintensities: relationship to amyloid and tau burden. *Brain*. 2019;142(8):2483-2491. doi:10.1093/brain/awz162
- Zhang J, Chen H, Wang J, et al. Linking white matter hyperintensities to regional cortical thinning, amyloid deposition, and synaptic density loss in Alzheimer's disease. *Alzheimers Dement*. 2024;20(6):3931-3942. doi:10.1002/alz.13845
- Barisano G, Iv M, Choupan J, et al. Robust, fully-automated assessment of cerebral perivascular spaces and white matter lesions: a multicentre MRI longitudinal study of their evolution and association with risk of dementia and accelerated brain atrophy. *eBioMed*. 2025;111:105523. doi:10.1016/j.ebiom.2024.105523
- Petit D, Fernández SG, Zoltowska KM, et al. A $\beta$  profiles generated by Alzheimer's disease causing PSEN1 variants determine the pathogenicity of the mutation and predict age at disease onset. *Mol Psychiatry*. 2022;27(6):2821-2832. doi:10.1038/s41380-022-01518-6
- Ryman DC, Acosta-Baena N, Aisen PS, et al. Symptom onset in autosomal dominant Alzheimer disease: a systematic

- review and meta-analysis. *Neurology*. 2014;83(3):253-260. doi:[10.1212/WNL.0000000000000596](https://doi.org/10.1212/WNL.0000000000000596)
8. Bateman RJ, Xiong C, Benzinger TLS, et al. Clinical and biomarker changes in dominantly inherited Alzheimer's disease. *N Engl J Med*. 2012;367(9):795-804. doi:[10.1056/NEJMoa1202753](https://doi.org/10.1056/NEJMoa1202753)
9. Lee S, Viqar F, Zimmerman ME, et al. White matter hyperintensities are a core feature of Alzheimer's disease: evidence from the dominantly inherited Alzheimer network. *Ann Neurol*. 2016;79(6):929-939. doi:[10.1002/ana.24647](https://doi.org/10.1002/ana.24647)
10. Gordon BA, Blazey TM, Su Y, et al. Spatial patterns of neuroimaging biomarker change in individuals from families with autosomal dominant Alzheimer's disease: a longitudinal study. *Lancet Neurol*. 2018;17(3):241-250. doi:[10.1016/S1474-4422\(18\)30028-0](https://doi.org/10.1016/S1474-4422(18)30028-0)
11. Fagan AM, Xiong C, Jasielec MS, et al. Longitudinal change in CSF biomarkers in autosomal-dominant Alzheimer's disease. *Sci Transl Med*. 2014;6(226):226ra30-226ra30. doi:[10.1126/scitranslmed.3007901](https://doi.org/10.1126/scitranslmed.3007901)
12. Wisch JK, McKay NS, Boerwinkle AH, et al. Comparison of tau spread in people with Down syndrome versus autosomal-dominant Alzheimer's disease: a cross-sectional study. *Lancet Neurol*. 2024;23(5):500-510. doi:[10.1016/S1474-4422\(24\)00084-X](https://doi.org/10.1016/S1474-4422(24)00084-X)
13. Shirzadi Z, Schultz SA, Yau WYW, et al. Etiology of white matter hyperintensities in autosomal dominant and sporadic Alzheimer disease. *JAMA Neurol*. 2023;80(12):1353. doi:[10.1001/jamaneurol.2023.3618](https://doi.org/10.1001/jamaneurol.2023.3618)
14. Joseph-Mathurin N, Feldman RL, Lu R, et al. Presenilin-1 mutation position influences amyloidosis, small vessel disease, and dementia with disease stage. *Alzheimers Dement*. 2024;20(4):2680-2697. doi:[10.1002/alz.13729](https://doi.org/10.1002/alz.13729)
15. Dering M, Biessels GJ, Brodtmann A, et al. Neuroimaging standards for research into small vessel disease—advances since 2013. *Lancet Neurol*. 2023;22(7):602-618. doi:[10.1016/S1474-4422\(23\)00131-X](https://doi.org/10.1016/S1474-4422(23)00131-X)
16. Barisano G, Lynch KM, Sibilia F, et al. Imaging perivascular space structure and function using brain MRI. *NeuroImage*. 2022;257:119329. doi:[10.1016/j.neuroimage.2022.119329](https://doi.org/10.1016/j.neuroimage.2022.119329)
17. Hadaczek P, Yamashita Y, Mirek H, et al. The "Perivascular Pump" driven by arterial pulsation is a powerful mechanism for the distribution of therapeutic molecules within the brain. *Mol Ther*. 2006;14(1):69-78. doi:[10.1016/j.ymthe.2006.02.018](https://doi.org/10.1016/j.ymthe.2006.02.018)
18. Iliff JJ, Wang M, Zeppenfeld DM, et al. Cerebral arterial pulsation drives paravascular CSF-interstitial fluid exchange in the murine brain. *J Neurosci*. 2013;33(46):18190-18199. doi:[10.1523/JNEUROSCI.1592-13.2013](https://doi.org/10.1523/JNEUROSCI.1592-13.2013)
19. Kress BT, Iliff JJ, Xia M, et al. Impairment of paravascular clearance pathways in the aging brain. *Ann Neurol*. 2014;76(6):845-861. doi:[10.1002/ana.24271](https://doi.org/10.1002/ana.24271)
20. van Veluw SJ, Hou SS, Calvo-Rodriguez M, et al. Vasomotion as a driving force for paravascular clearance in the awake mouse brain. *Neuron*. 2020;105(3):549-561.e5. doi:[10.1016/j.neuron.2019.10.033](https://doi.org/10.1016/j.neuron.2019.10.033)
21. Mestre H, Tithof J, Du T, et al. Flow of cerebrospinal fluid is driven by arterial pulsations and is reduced in hypertension. *Nat Commun*. 2018;9(1):4878. doi:[10.1038/s41467-018-07318-3](https://doi.org/10.1038/s41467-018-07318-3)
22. Bown CW, Carare RO, Schrag MS, Jefferson AL. Physiology and clinical relevance of enlarged perivascular spaces in the aging brain. *Neurology*. 2022;98(3):107-117. doi:[10.1212/WNL.00000000000013077](https://doi.org/10.1212/WNL.00000000000013077)
23. Ringman JM, Monsell S, Ng DW, et al. Neuropathology of autosomal dominant Alzheimer disease in the National Alzheimer Coordinating Center database. *J Neuropathol Exp Neurol*. 2016;75(3):284-290. doi:[10.1093/jnen/nlv028](https://doi.org/10.1093/jnen/nlv028)
24. Sepulveda-Falla D, Villegas Lanau CA, White iii C, et al. Comorbidities in early-onset sporadic versus presenilin-1 mutation-associated Alzheimer disease dementia: evidence for dependency on Alzheimer disease neuropathological changes. *J Neuropathol Exp Neurol*. 2025;84(2):104-113. doi:[10.1093/jnen/nlae122](https://doi.org/10.1093/jnen/nlae122)
25. Littau JL, Velilla L, Hase Y, et al. Evidence of beta amyloid independent small vessel disease in familial Alzheimer's disease. *Brain Pathol*. 2022;32(6):e13097. doi:[10.1111/bpa.13097](https://doi.org/10.1111/bpa.13097)
26. Schoemaker D, Zanon Zotin MC, Chen K, et al. White matter hyperintensities are a prominent feature of autosomal dominant Alzheimer's disease that emerge prior to dementia. *Alz Res Ther*. 2022;14(1):89. doi:[10.1186/s13195-022-01030-7](https://doi.org/10.1186/s13195-022-01030-7)
27. Schultz SA, Liu L, Schultz AP, et al.  $\gamma$ -Secretase activity, clinical features, and biomarkers of autosomal dominant Alzheimer's disease: cross-sectional and longitudinal analysis of the dominantly inherited Alzheimer network observational study (DIAN-OBS). *Lancet Neurol*. 2024;23(9):913-924. doi:[10.1016/S1474-4422\(24\)00236-9](https://doi.org/10.1016/S1474-4422(24)00236-9)
28. Fischl B. FreeSurfer. *Neuroimage*. 2012;62(2):774-781. doi:[10.1016/j.neuroimage.2012.01.021](https://doi.org/10.1016/j.neuroimage.2012.01.021)
29. Frangi AF, Niessen WJ, Vincken KL, Viergever MA. Multiscale vessel enhancement filtering. In: Wells WM, Colchester A, Delp S, eds. *Medical Image Computing and Computer-Assisted Intervention – MICCAI'98*. Springer; 1998:130-137. doi:[10.1007/BFb0056195](https://doi.org/10.1007/BFb0056195)
30. Puonti O, Iglesias JE, Van Leemput K. Fast and sequence-adaptive whole-brain segmentation using parametric Bayesian modeling. *NeuroImage*. 2016;143:235-249. doi:[10.1016/j.neuroimage.2016.09.011](https://doi.org/10.1016/j.neuroimage.2016.09.011)
31. Araque Caballero MÀ, Suárez-Calvet M, Dering M, et al. White matter diffusion alterations precede symptom onset in autosomal dominant Alzheimer's disease. *Brain*. 2018;141(10):3065-3080. doi:[10.1093/brain/awy229](https://doi.org/10.1093/brain/awy229)
32. Lynch KM, Sepelband F, Toga AW, Choupan J. Brain perivascular space imaging across the human lifespan. *NeuroImage*. 2023;271:120009. doi:[10.1016/j.neuroimage.2023.120009](https://doi.org/10.1016/j.neuroimage.2023.120009)
33. Jia J, Ning Y, Chen M, et al. Biomarker changes during 20 years preceding Alzheimer's Disease. *N Engl J Med*. 2024;390(8):712-722. doi:[10.1056/NEJMoa2310168](https://doi.org/10.1056/NEJMoa2310168)
34. Klunk WE, Price JC, Mathis CA, et al. Amyloid deposition begins in the striatum of presenilin-1 mutation carriers from two unrelated pedigrees. *J Neurosci*. 2007;27(23):6174-6184. doi:[10.1523/JNEUROSCI.0730-07.2007](https://doi.org/10.1523/JNEUROSCI.0730-07.2007)
35. McDade E, Kim A, James J, et al. Cerebral perfusion alterations and cerebral amyloid in autosomal dominant Alzheimer disease. *Neurology*. 2014;83(8):710-717. doi:[10.1212/WNL.0000000000000721](https://doi.org/10.1212/WNL.0000000000000721)
36. Drachman DA, Smith TW, Alkamachi B, Kane K. Microvascular changes in Down syndrome with Alzheimer's-type pathology: insights into a potential vascular mechanism for Down syndrome and Alzheimer's disease. *Alzheimers Dement*. 2017;13(12):1389-1396. doi:[10.1016/j.jalz.2017.05.003](https://doi.org/10.1016/j.jalz.2017.05.003)
37. Sepelband F, Barisano G, Sheikh-Bahaei N, et al. Volumetric distribution of perivascular space in relation to mild cognitive impairment. *Neurobiol Aging*. 2021;99:28-43. doi:[10.1016/j.neurobiolaging.2020.12.010](https://doi.org/10.1016/j.neurobiolaging.2020.12.010)
38. Wardlaw JM, Benveniste H, Nedergaard M, et al. Perivascular spaces in the brain: anatomy, physiology and pathology. *Nat Rev Neurol*. 2020;16(3):137-153. doi:[10.1038/s41582-020-0312-z](https://doi.org/10.1038/s41582-020-0312-z)
39. Peng W, Acharyar TM, Li B, et al. Suppression of glymphatic fluid transport in a mouse model of Alzheimer's disease. *Neurobiol Dis*. 2016;93:215-225. doi:[10.1016/j.nbd.2016.05.015](https://doi.org/10.1016/j.nbd.2016.05.015)
40. Kim SH, Ahn JH, Yang H, Lee P, Koh GY, Jeong Y. Cerebral amyloid angiopathy aggravates perivascular clearance impairment in an Alzheimer's disease mouse model. *Acta Neuropathol Commun*. 2020;8:181. doi:[10.1186/s40478-020-01042-0](https://doi.org/10.1186/s40478-020-01042-0)
41. Suárez-Calvet M, Araque Caballero MÀ, Kleinberger G, et al. Early changes in CSF sTREM2 in dominantly inherited Alzheimer's disease occur after amyloid deposition and neuronal injury. *Sci Transl Med*. 2016;8(369):369ra178-369ra178. doi:[10.1126/scitranslmed.aag1767](https://doi.org/10.1126/scitranslmed.aag1767)
42. Wuerfel J, Haertle M, Waiczies H, et al. Perivascular spaces—MRI marker of inflammatory activity in the brain? *Brain*. 2008;131(9):2332-2340. doi:[10.1093/brain/awn171](https://doi.org/10.1093/brain/awn171)
43. Ge Y, Law M, Herbert J, Grossman RI. Prominent perivenular spaces in multiple sclerosis as a sign of perivascular inflammation in primary demyelination. *AJNR Am J Neuroradiol*. 2005;26(9):2316-2319.

44. Ineichen BV, Okar SV, Proulx ST, Engelhardt B, Lassmann H, Reich DS. Perivascular spaces and their role in neuroinflammation. *Neuron*. 2022;110(21):3566-3581. doi:[10.1016/j.neuron.2022.10.024](https://doi.org/10.1016/j.neuron.2022.10.024)
45. Ringman JM, Sachs MC, Zhou Y, Monsell SE, Saver JL, Vinters HV. Clinical predictors of severe cerebral amyloid angiopathy and influence of APOE genotype in persons with pathologically verified Alzheimer disease. *JAMA Neurol*. 2014;71(7):878-883. doi:[10.1001/jamaneurol.2014.681](https://doi.org/10.1001/jamaneurol.2014.681)
46. Zhao M, Li Y, Han X, et al. Association of enlarged perivascular spaces with cognitive function in dementia-free older adults: a population-based study. *Alzheimers Dement*. 2024;16(3):e12618. doi:[10.1002/dad2.12618](https://doi.org/10.1002/dad2.12618)
47. Gogniat MA, Khan OA, Bown CW, et al. Perivascular space burden interacts with APOE-ε4 status on cognition in older adults. *Neurobiol Aging*. 2024;136:1-8. doi:[10.1016/j.neurobiolaging.2024.01.002](https://doi.org/10.1016/j.neurobiolaging.2024.01.002)

## SUPPORTING INFORMATION

Additional supporting information can be found online in the Supporting Information section at the end of this article.

**How to cite this article:** Leone R, Kobeleva X, Rowe B, Choupan J, Ringman JM, Barisano G. Alterations in MRI-visible perivascular spaces precede dementia diagnosis by 18 years in autosomal dominant Alzheimer's disease. *Alzheimer's Dement*. 2025;:e70588. <https://doi.org/10.1002/alz.70588>